

RESEARCH

Open Access



# Finite Element Analysis and Calculation Method of Residual Flexural Capacity of Post-fire RC Beams

Bin Cai<sup>1,2</sup>, Bo Li<sup>1</sup> and Feng Fu<sup>2\*</sup>

## Abstract

Fire tests and subsequent bending tests of four reinforced concrete (RC) beams were performed. Based on these tests, the post-fire performance of RC beams was further studied using finite-element simulation through reasonable selection of suitable thermal and thermodynamic parameters of steel and concrete materials. A thermodynamic model of RC beams with three sides under fire was built using finite-element analysis (FEA) software ABAQUS. The FEA model was validated with the results of fire tests. Different factors were taken into account for further parametric studies in fire using the proposed FE model. The results show that the main factors affecting the fire resistance of the beams are the thickness of the concrete cover, reinforcement ratio of longitudinal steel, the fire exposure time and the fire exposure sides. Based on the strength reduction formula at high temperature of steel and concrete and four test results, an improved section method was proposed to develop a calculation formula to calculate the flexural capacity of RC beams after fire. The theoretical calculation method proposed in this paper shows good agreement with FEA results, which can be used to calculate the flexural capacity of RC beams after fire.

**Keywords:** Post-fire, reinforced concrete beams, finite element, ABAQUS, theoretical calculation

## 1 Introduction

Reinforced concrete (RC), as one of the major building materials of modern architectural structures, will form nonuniform temperature fields after exposure to fire (Shao et al. 2003; Cheng 2007). The thermal stress and expansion (Zhao 2014) due to fire will lead to stress redistribution of overall structures and reduction of structural flexural capacity or even the local structural destabilization, which further induce the collapse of overall structures and bring about massive losses to the possessions and life of humans (Ban 2008). Thus, the temperature fields should be determined first for subsequent analysis of RC structures to understand the degradation in the mechanical properties and flexural capacity after exposure to fire, which are the keys to evaluate

whether the RC structures can be used anymore (Tian 2002; Zeng 2006). So far, there is considerable research in the aspect of test and finite-element analysis (FEA). Fu et al. (2015) studied how the fire surfaces of RC beams affected the temperature fields. Liao et al. (2013) designed the shear tests and a FEA method was proposed to calculate the shear flexural capacity among one room temperature and seven post-fire RC beams, which has the accepted accuracy. Sun et al. (2002) investigated the mechanical performances in the tensile region and the compressive region of beam sections at elevating temperature and after cooling. Shi and Guo (2000) tested the structural performances of RC beams at high temperature and presented the temperature distributions of beam sections, a coupling temperature–stress constitutive law of concrete and the main performances at different surfaces after fire exposure. Lu et al. (1993) studied the 1-, 2- and 3-surface fire exposure of 12 RC simply-supported beams, presented the bending moment–curvature relations in different temperature fields and computationally

\*Correspondence: feng.fu.1@city.ac.uk

<sup>2</sup> School of Mathematics, Computer Science and Engineering, City, University of London, London, UK

Full list of author information is available at the end of the article  
Journal information: ISSN 1976-0485 / eISSN 2234-1315

validated the load–deflection relations of RC beams. El-Hawary et al. (1997) investigated the mechanical behavior of post-fire RC beams in the shear zone by the method of test. Parthasarathi et al. (2019) carried out experimental research on 10 RC short columns at different temperatures, obtained the deflection, stiffness and variation of the specimen at high temperature, and compared the experimental results with the FEA results. The results were reasonably well. Kodur and Agrawal (2017) studied the fire response of RC beams caused by temperature-induced bond degradation and an FEA was developed. Fu (2016a) developed 3D FE modelling approach using ABAQUS. Fu (2020) developed a machine learning algorithm for fire safety design. Eamon and Jensen (2013) conducted a reliability analysis of RC columns subjected to fire, and various factors such as the fire type, load ratio, reinforcement ratio, concrete cover, concrete strength were considered in the analysis. Xu et al. (2015) conducted a fire endurance test of 6 high strength steel RC continuous T-beams and confirmed the feasibility of designing high strength steel RC continuous T-beams using plastic analysis. Hassan et al. (2019) designed an experiment to investigate the effect of different retrofitting techniques on the performance of concrete at different temperature on 31 beams. Chen et al. (2009) carried out experimental research on the mechanical properties of 9 full-size concrete columns. The results showed that with the increase of fire time, the residual flexural capacity decreases. Mathew and Joseph (2018) studied the flexural behavior of fly ash geopolymer concrete beams at different temperature. The results showed that the deformation characteristic of geopolymer concrete beams is similar to that of the reinforced cement concrete beams at ambient temperature, but big difference noticed at high temperature. Di Capua and Mari (2007) proposed two models, the thermal model and the mechanical model, for calculating the RC beams exposed to fire, which were in good agreement with test results. Bratina et al. (2003) explored the post-fire nonlinear structural analysis of RC beams. In theory, Xiang et al. (2010) studied the calculation method of flexural capacity for fire-damaged RC bending members, Yu et al. (2005a, b) studied the effects of different factors on the mechanical properties of concrete exposed to high temperature and proposed the equations of stress–strain relation for various concrete after high temperature. Hu et al. (2006) established estimation methods for the flexural capacity of slabs subjected to fire and axially loaded concrete square columns subjected to fire on four surfaces. Lie and Irwin (1993) described a method for the calculation of the fire resistance of RC columns with rectangular cross sections. Jiang et al. (2008) discussed the rectangle beam with single reinforcement, and proposed a method to calculate the residual capacity of the RC member.

Based on above research, it can be seen that, most scholars' research primarily focusses on the constitutive

relationship of materials during or after fire, as well as the response analysis and damage assessment, and the flexural capacity of theoretical calculation of the post-fire RC beams is barely investigated. In addition, the major factor affecting the behaviour of the RC beams in fire is not well investigated. The 500 °C isotherm method specified in Eurocode (BSI 2004) is the most widely used theoretical calculation method for the residual bearing capacity of RC beams after fire. The method is based on the assumption that concrete above 500 °C does not provide load-bearing capacity to members, while concrete within 500 °C is considered to maintain its initial values of strength and elastic modulus. However, this method is a rough calculation method cannot accurately evaluate the structures after fire. BS 5950: Part 8 (2003) specifies a calculation method of the fire resistance of members in bending which is called 'moment capacity method' or called "section method". It is used primarily for steel sections but concrete members. Therefore, RC beams fire tests and subsequent bending test were performed in this paper, based on the test results and the existing moment capacity method, a new theoretical calculation model using improved section method to calculate the flexural capacity of the post-fire beams. The model first conducts heat transfer analysis to obtain the temperature field of the beam section, and then divides the beam section to small divisions and obtain the average temperature of each divisions. Finally, based on the material strength reduction formulas in fire, the flexural capacity can be accurately obtained for RC beam after fire. Compared with the 500 °C isotherm method, the advantage of this method is that it fully considers the changes of the temperature field and accurately considers the changes of the material strength caused by the temperature changes in each micro area, and the results obtained are more accurate. The accuracy of the theoretical calculation is validated through the comparison with simulation and test results, which offers a new way for the evaluation of post-fire RC structures. In addition, a thermodynamic model of RC beams with three sides under fire was built using finite-element analysis (FEA) software ABAQUS. The FEA model was validated with the results of fire tests. Different factors were taken into account for further parametric studies in fire using the proposed FE model.

## 2 Research Methodology

For evaluating post-fire residual flexural capacity of RC beams, three approaches are adopted: experiment investigate (fire tests and post-fire static load tests) of RC beams (stage 1), numerical analysis of RC beams on the basis of Finite-Element software (stage 2) and finally, theoretical analysis of residual flexural capacity on the basis of improved section method (stage 3). A flow chart in Fig. 1 illustrates the three stages for evaluating residual strength of fire-exposed RC beams.

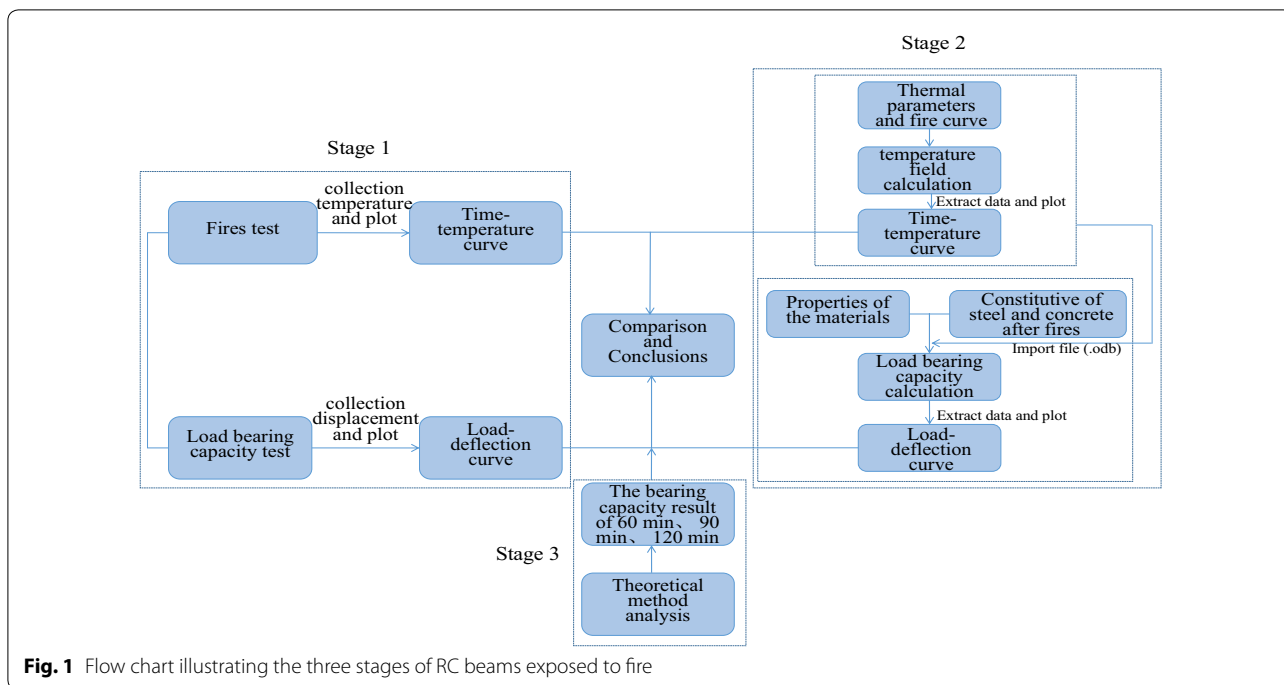


**Fig. 1** Flow chart illustrating the three stages of RC beams exposed to fire

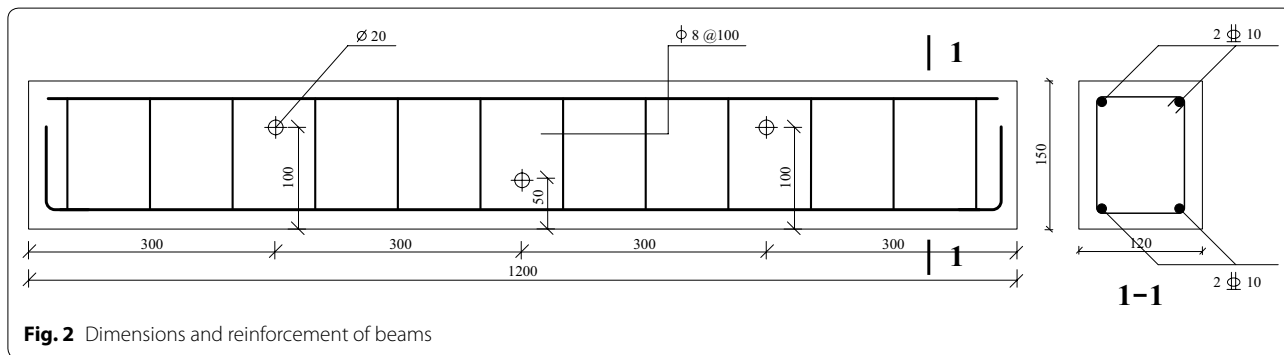


**Fig. 2** Dimensions and reinforcement of beams

### 3 Fire and Bending Tests of RC Beams

#### 3.1 Fire Tests

##### 3.1.1 Test Preparations

The experiments were conducted in the Structure Laboratory of Jilin Jianzhu University. 4 RC beams were fabricated with dimensions and reinforcement details shown in Fig. 2. The mix proportion of concrete (Table 1) is W:C:S:G=0.38:1:1.11:2.72. The basic parameters of the reinforcement are shown in Table 2. Two of them were exposed to 60 min high temperature in a furnace (Table 3). The temperature distribution of the beams subjected to fire were, therefore, obtained, which provides a comparison for the subsequent numerical analysis.

To record the temperature changes during the experiments, thermocouples were embedded into the pre-drilled holes of the beams F1 and F2 and filled with cement mortar.

**Table 1** Mix proportion of concrete

Water (Kg)	Cement (Kg)	Sand (Kg)	Gravel (Kg)
175	461	512	1252

Then the beams were covered with fireproofing cotton at locations shown in Fig. 3 to simulate 3-sided fire exposure.

##### 3.1.2 Test Observations

The two beams were placed into a furnace (Fig. 4) for 60 min fire exposure. During the heating stage of the members, when the exposure time is 12 min, a small amount of water vapor can be seen on the beam surface from the observation hole in the furnace. When the exposure time is 21 min, a large

**Table 2 Basic parameters of the reinforcement**

Type of reinforcement	Specification of steels	Yield strength (N/mm <sup>2</sup> )	Ultimate strength (N/mm <sup>2</sup> )	Elastic modulus (× 10 <sup>5</sup> N/mm <sup>2</sup> )
Pulled	HRB400	469	583	2.05
Compressed	HRB400	469	583	2.05
Stirrup	HPB300	346	431	2.13

**Table 3 Basic parameters of specimens**

Specimen No.	Concrete strength grade	Test conditions	Fire exposure time (min)
N1	C30	Room-temperature static test	–
N2	C30	Room-temperature static test	–
F1	C30	Post-fire static test	60
F2	C30	Post-fire static test	60

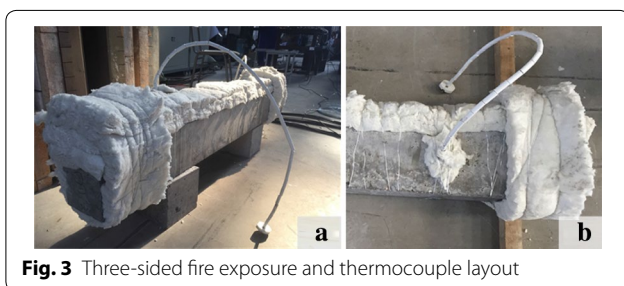


**Fig. 3** Three-sided fire exposure and thermocouple layout

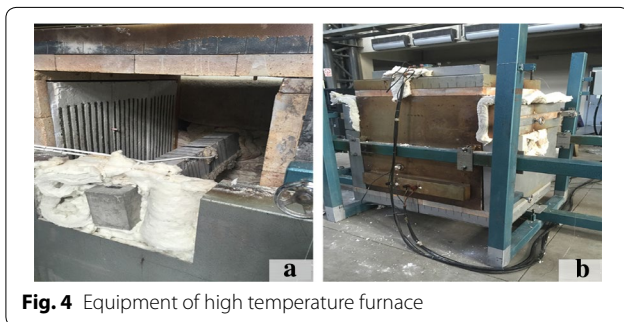


**Fig. 4** Equipment of high temperature furnace

amount of water vapor volatilizes from the furnace, and the water vapor is the most vigorous when it is 27 min. As the exposure time increases, the water vapor in the furnace gradually decreases. When the exposure time is 42 min, the water vapor in the furnace basically disappears. The main reason for this phenomenon is that some of the free water inside the beam and the small amount of water gel evaporated at the beginning of the fire. As the temperature in the furnace increases, a large amount of free water and water gel begin to volatilize. At the same time, the beam is dehydrated in a large

amount, and when the water vapor in the furnace is substantially disappeared, the beam is completely dehydrated.

When the RC beams are dehydrated at high temperature, the sound of slight cracking as well as a frequent slight popping can be heard. A large number of diagonal cracks are noticed on the surface of the beam when it is taken out from the furnace after tests, and the longer the exposure time is, the more larger the crack is. From the overall point of view, there are phenomena such as peeling, outer drum, and crispness, and the surface color changes from normal color to light yellow or even dark yellow. The reason for this phenomenon is that during the process of the fire, some complicated chemical reactions occur inside the beam, such as the decomposition of Ca(OH)<sub>2</sub> and minerals of aggregate, which cause certain damage to the interior of the beam. The internal expansion of the beam causes surface cracking.

**3.1.3 Test Results and Analysis**

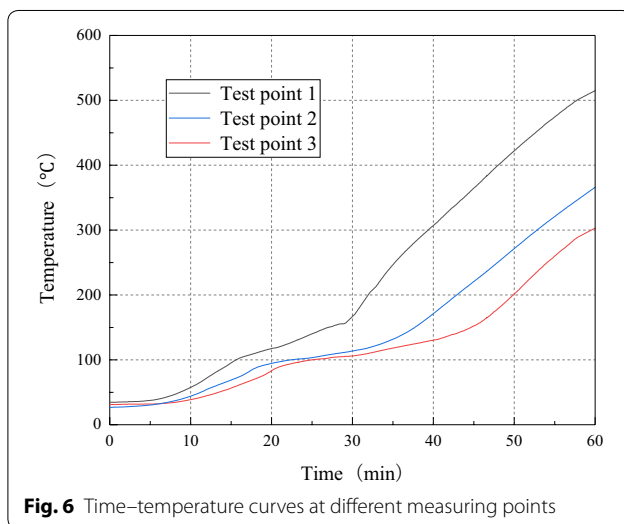
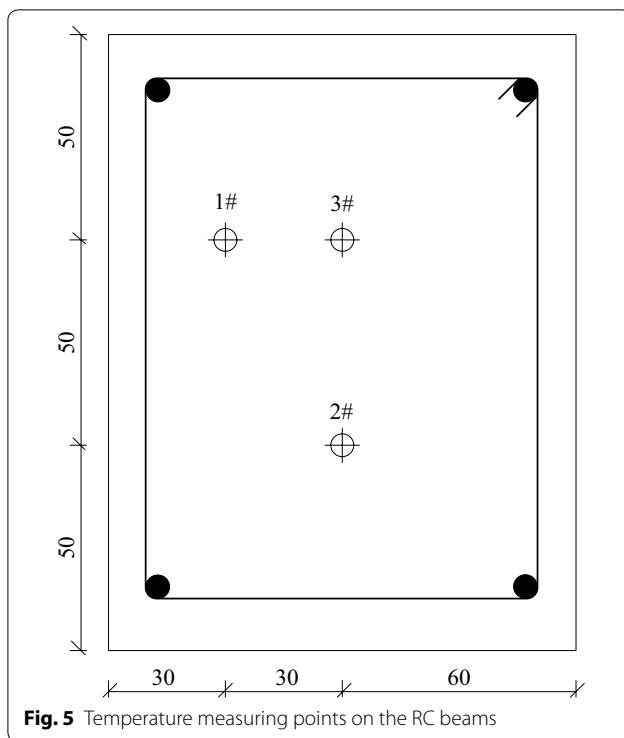
Three temperature measuring points are set on each specimen (Fig. 5). The time–temperature curves (Fig. 6) of the three temperature measuring points of each beam section after 60 min of fire are obtained from the above beam tests. Due to the thermal inertia of concrete, the temperature distribution of the section is uneven after fire, and the temperature gradient is larger near the furnace. The temperature is generally rising, but it can be seen from the figure that there is a temperature platform at about 120 °C, which may due to the evaporation of water in the beam causing partial heat loss.

**3.2 Static Tests**

After fire tests, the two beams were cooled to room temperature, then, static tests were performed. The effects of fire exposure time on the flexural capacity of the beam were, therefore, investigated. In brief, 2 none-fire-exposed beams and 2 post-fire beams were tested using a 4-point bending test rigs, as it is shown in Fig. 7. The instrumentations are shown in Fig. 7.

**3.2.1 Test Phenomena**

Under the vertical load, the displacement of the RC beams gradually increases with the increase of the load. After a period of loading, tiny hairline cracks can be seen first in the mid-span of the beam. The crack l developed slowly and upward, and new vertical cracks appeared



on both sides of the mid-span under the constant load. As the loading continued, the cracks gradually become longer, and the gaps become larger. After that, the displacement of the beam becomes larger and the load

remained basically unchanged. After a while, the load drop rapidly, until the failure of the beam.

### 3.2.2 Test Results and Discussion

The load–deflection curves of the 4 beams are plotted in Fig. 8. Clearly, during the loading of the RC beams, the mid-span load–deflection relation first increased proportionally. When the load reached certain value, it did not increase any more, and the curve reached yield stage. Then the load dropped abruptly, and the beams failed. The curves showed the flexural capacity was weakened by about 30% after the fire exposure.

## 4 Finite-Element Modelling

To be able to simulate the response of the RC beams after fire, a sequential Thermal–Mechanical Coupling approach is implemented in ABAQUS modelling. The heat transferring analysis was performed first to get the temperature distribution. The thermal result then input into the mechanical model for further mechanical analysis.

### 4.1 Basic Assumptions

Some basic assumptions were proposed to simplify the simulation:

1. The concrete strength of different mesh in the compression zone is different, but the strength in each mesh is regarded as a constant;
2. The equivalent reduction coefficient of the concrete strength of the entire compression zone can be obtained by weighting the average of the cross-sectional compression zone area;
3. The heat loss due to moisture evaporation during the fire was not considered;
4. There was no bonding slip between the reinforcement and concrete.

### 4.2 Heat Transfer Analysis

#### 4.2.1 Thermal Properties of the Materials

To obtain temperature fields of RC beams, heat transfer analysis was performed using ABAQUS. The specific heat capacity, thermal conductivity, and density of the materials should be first determined, which are the basis for the analysis. The parameters were selected based on Wang and He (2009).

The thermal conductivity of concrete  $\lambda_{cT}$  ( $W/(m \text{ } ^\circ C)$ ) is

$$\lambda_{cT} = 2 - 0.24 \left( \frac{T}{120} \right) + 0.012 \left( \frac{T}{120} \right)^2 \quad (20^\circ C \leq T \leq 1200^\circ C), \quad (1)$$

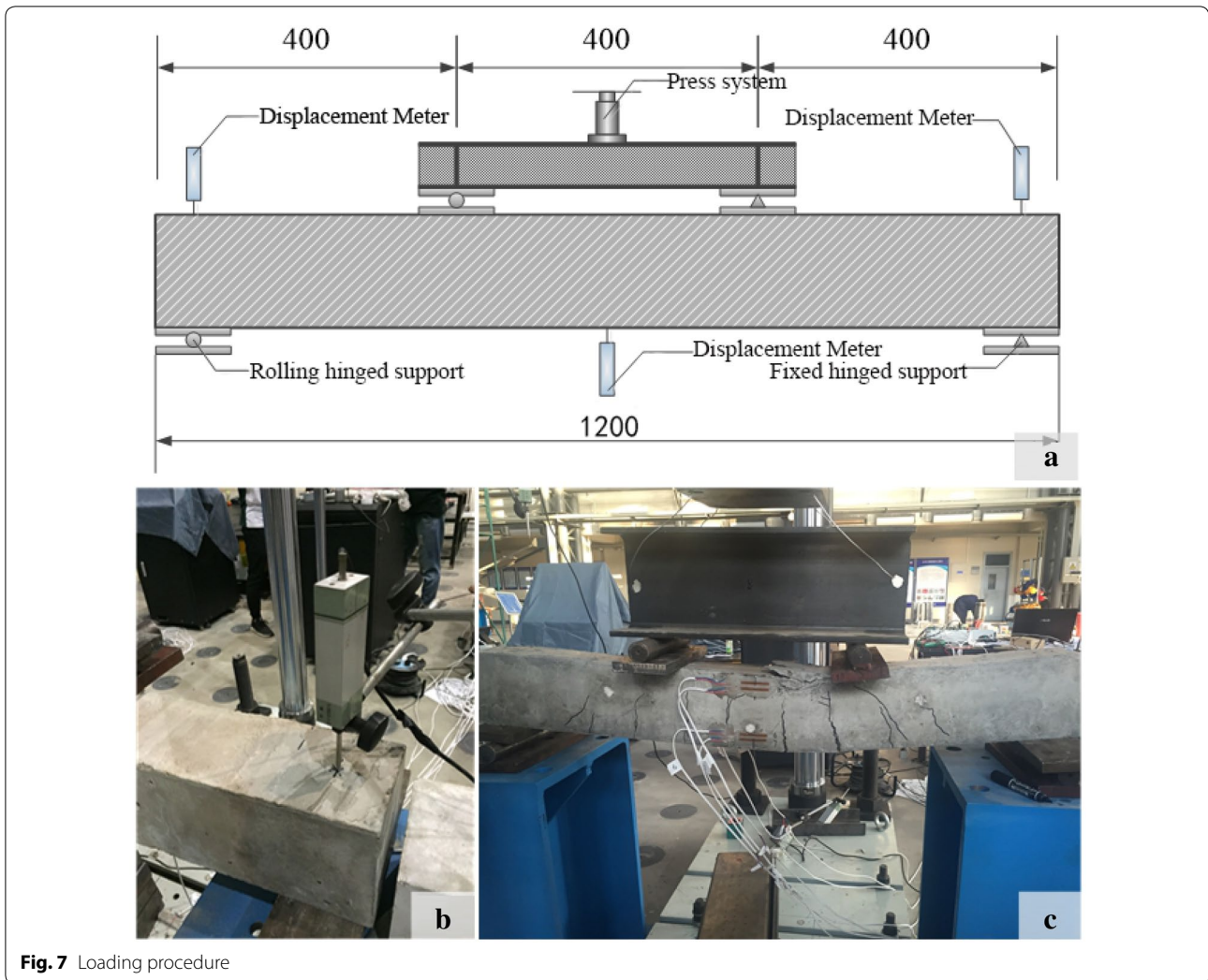


**Fig. 7** Loading procedure

where  $T$  is the temperature, °C.

The specific heat capacity of concrete  $C_{cT}$  (J/(Kg °C)) is

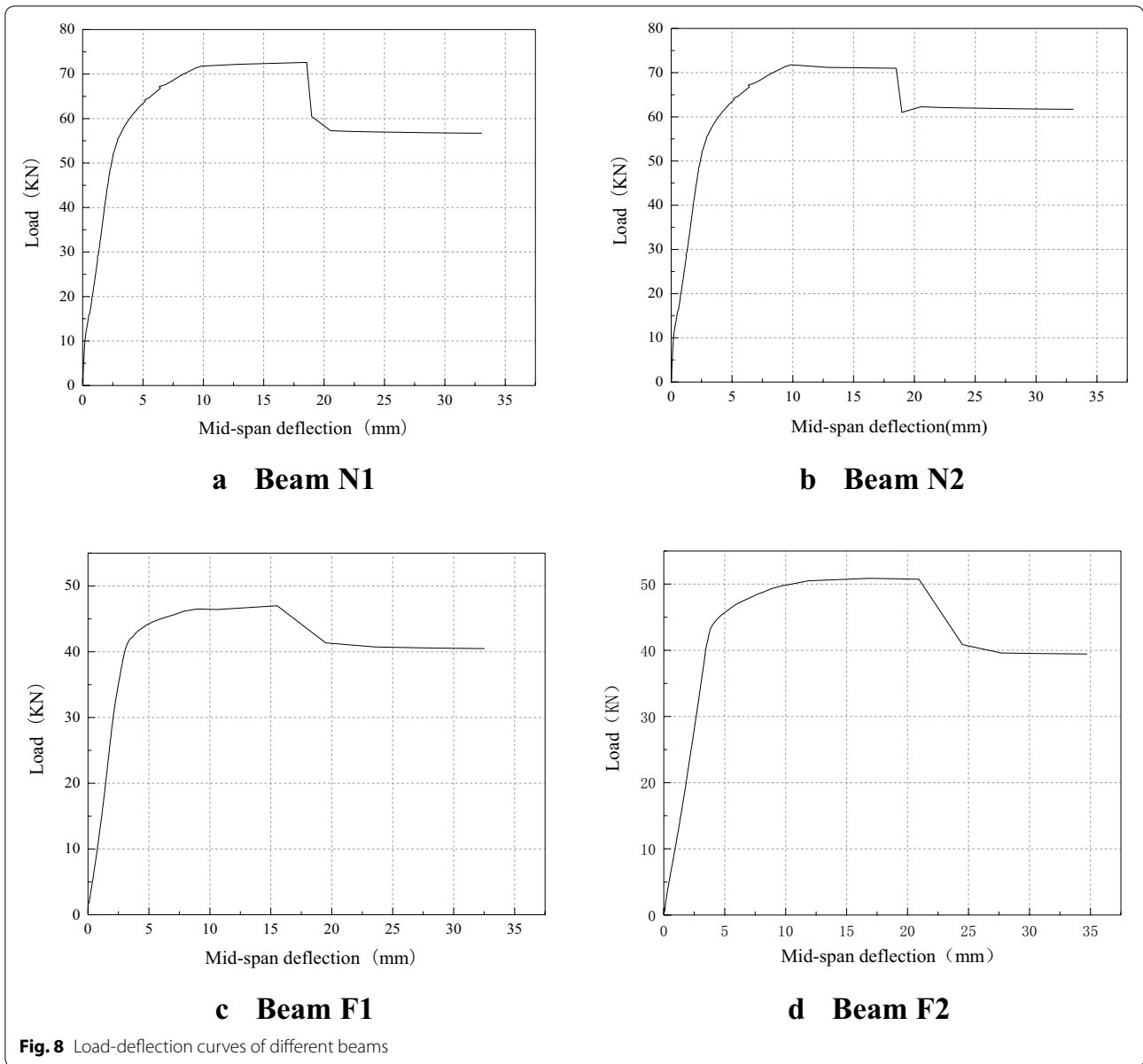
$$\lambda_{sT} = \begin{cases} 54 - 3.33 \times 10^{-2}T & (20^\circ\text{C} \leq T < 800^\circ\text{C}) \\ 27.3 & (800^\circ\text{C} \leq T \leq 1200^\circ\text{C}) \end{cases} \quad (3)$$

$$C_{cT} = 900 + 80 \left( \frac{T}{120} \right) - 4 \left( \frac{T}{120} \right)^2 \quad (20^\circ\text{C} \leq T \leq 1200^\circ\text{C}). \quad (2)$$

The thermal conductivity of reinforcement steel  $\lambda_{sT}$  (W/(m °C)) is

The specific heat capacity of reinforcement  $C_{sT}$  (J/(Kg °C)) is

$$C_{sT} = \begin{cases} 425 + 7.73 \times 10^{-1}T - 1.69 \times 10^{-3}T^2 + 2.22 \times 10^{-6}T^3 & (20^\circ\text{C} \leq T < 600^\circ\text{C}) \\ 666 + \frac{13002}{738-T} & (600^\circ\text{C} \leq T < 735^\circ\text{C}) \\ 545 + \frac{17820}{T-731} & (735^\circ\text{C} \leq T < 900^\circ\text{C}) \\ 650 & (900^\circ\text{C} \leq T \leq 1200^\circ\text{C}) \end{cases} \quad (4)$$



#### 4.2.2 Fire Temperature Curve

The heat transfer analysis was performed on the basis of a heating curve. Here the ISO-834 fire curve from the International Organization (ISO 1999) is adopted (Fig. 9). The curve can be expressed as (Fu 2016b,2018)

$$T = T_0 + 345 \lg(8t + 1), \tag{5}$$

where  $t$  is the heating time (min);  $T_0$  is the initial room temperature ( $^{\circ}\text{C}$ , which is  $20^{\circ}\text{C}$  here).

#### 4.2.3 FE Model Setup

A 3D finite-element model is built, as shown in Fig. 10. The concrete was simulated as DC3D8 8-node (Fu et al.

2010) linear heat transfer units, and the reinforcement steel as DC1D2 2-node heat transfer link units. The contact between reinforcement and concrete was simulated using Embedded Region. The beams were exposed to fire on three sides, and the modes of heat transfer in the fire-exposed faces were surface radiation and surface film condition, and the unfired faces were surface film condition. The thermal parameters of the materials were calculated according to Eqs. (1) to (4). After the heat transfer analysis steps and boundary conditions were set up, the models were meshed into cells in size of 10 mm. The temperature distribution of RC beam exposed to fire is shown in Fig. 10, the temperature field nephogram

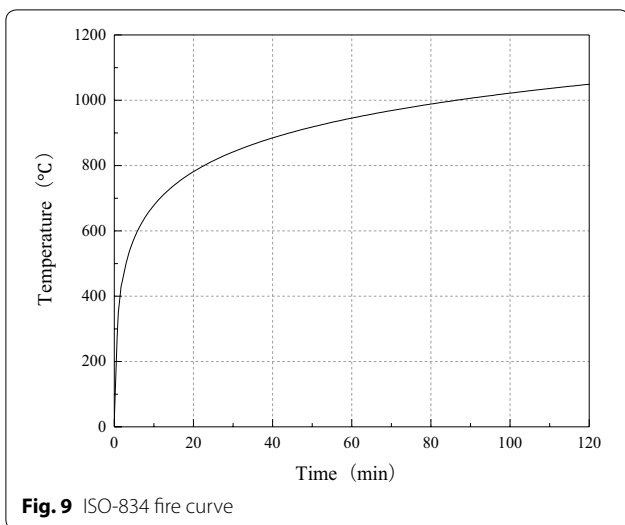


**Fig. 9** ISO-834 fire curve

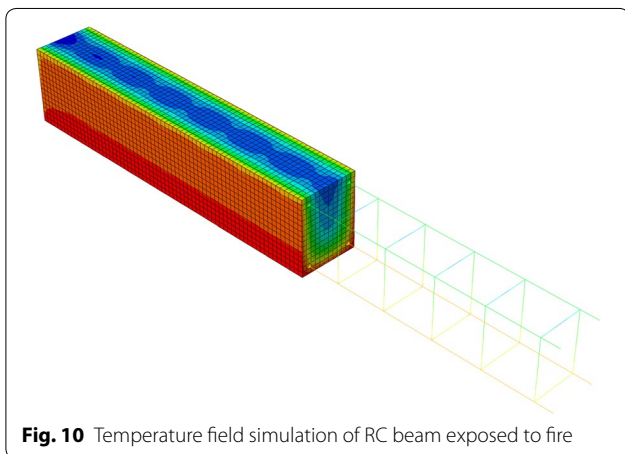


**Fig. 10** Temperature field simulation of RC beam exposed to fire

(Fig. 11) and the simulated results (Fig. 12) were shown as follows.

**4.2.4 FE Model Validation**

The temperature fields of post-fire RC beams obtained using ABAQUS is compared with test results, which can be visually observed. The simulated results were basically consistent with the test results.

**4.3 Static Analysis Procedure**

The degradation of the compressive strength of concrete, the yield strength of steel at high temperature were related to the maximum temperature. To be consistent with the test conditions, the temperature field simulation was performed first to determine the strength degradation of the materials, then the static load simulation was carried out. The mechanical performances

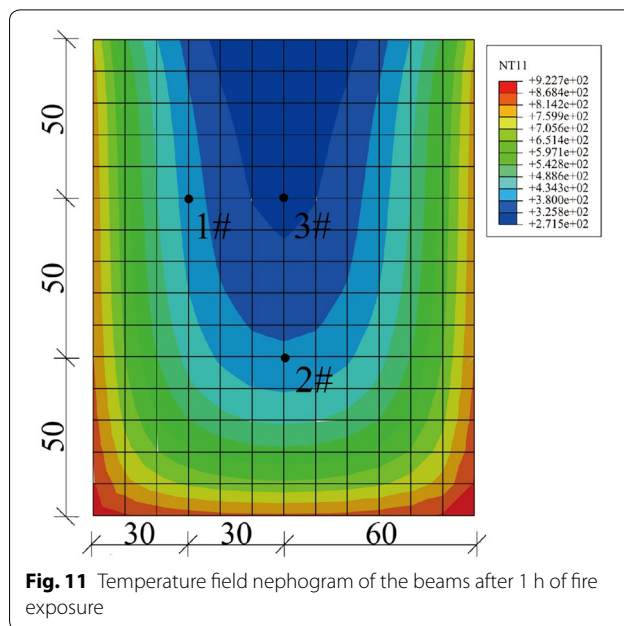


**Fig. 11** Temperature field nephogram of the beams after 1 h of fire exposure

of reinforcement or concrete varied with the change of maximum temperature, so the relations with temperature should be considered to determine the post-fire mechanical performances. They are determined according to the formula introduced in the following section.

**4.3.1 Constitutive Model of Concrete Under High Temperature**

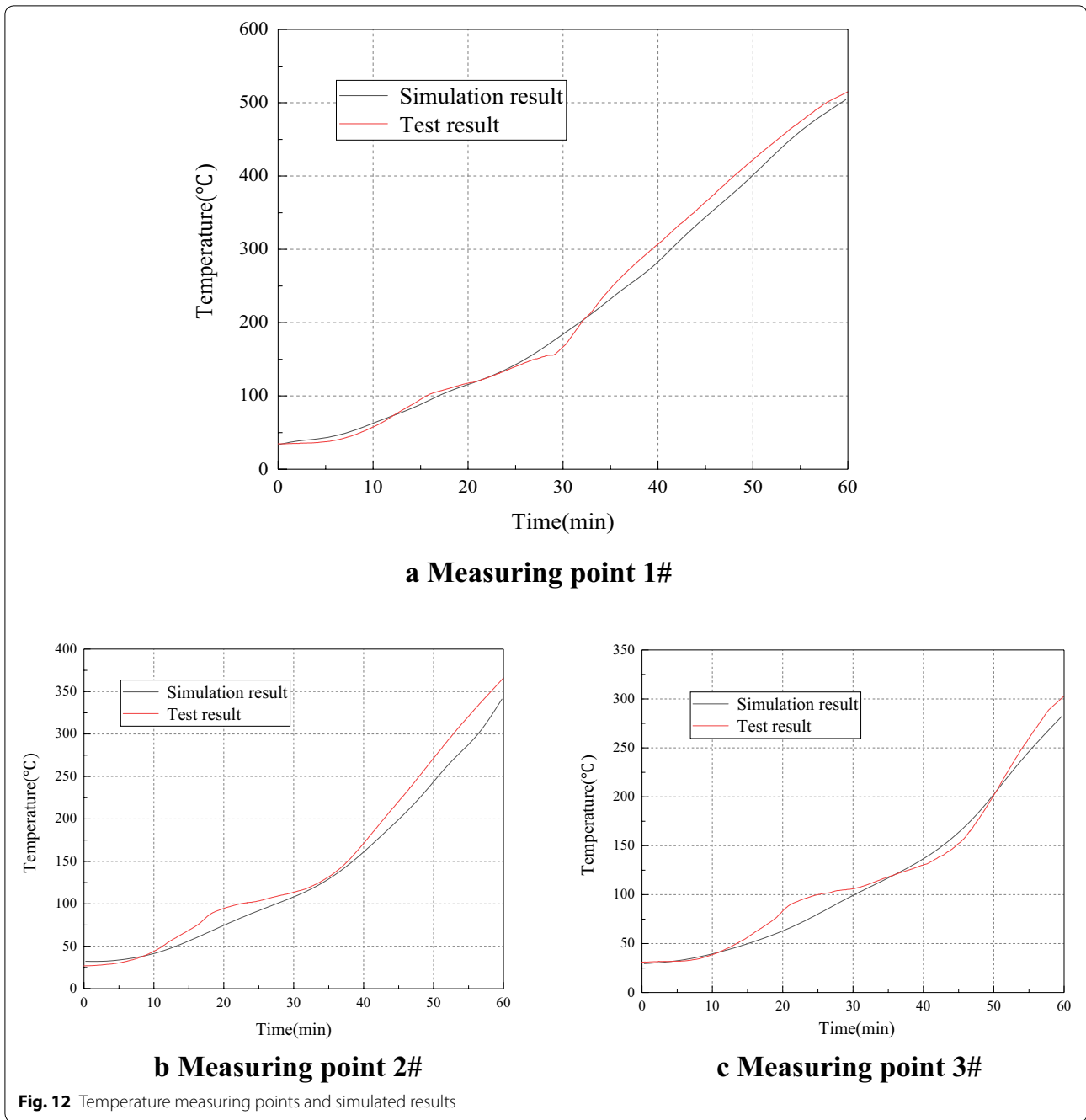
The post-fire mechanical properties of concrete were related to the fire exposure time, way of cooling, and type of skeletal materials. Here the model of post-fire concrete proposed by Yu et al. (2005a, b) was used. The compression stress–strain model (Fig. 13) of post-fire concrete can be determined according to formulas 7 and 8. The reduction factor of axial compressive strength of concrete with temperature change is shown in Fig. 14 according to formula 6.

The strength reduction factor of post-fire concrete  $\Psi_{cT}$  at  $T^{\circ}\text{C}$  is

$$\Psi_{cT} = \frac{f_c(T)}{f_c} = \frac{1}{1 + 9 \times [(T - 20)/800]^{c_1}}, \quad (6)$$

where  $f_c(T)$  is the axial compressive strength of concrete at high temperature,  $\text{N}/\text{mm}^2$ ;  $f_c$  is the axial compressive strength of concrete at room temperature,  $\text{N}/\text{mm}^2$ ;  $c_1$  is the parameter. (which is 3.55 here for ordinary concrete), for high-performance concrete (HPC) concrete  $c_1 = 6.70$ .





The compression peak strain of post-fire concrete  $\varepsilon_0(T)$  at  $T$  °C is

$$\varepsilon_0(T) = \left\{ 1 + c_4 \left[ \frac{(T - 20)}{100} \right]^2 \right\} \varepsilon_0, \quad (7)$$

where  $\varepsilon_0$  is the compressive strain of concrete at room temperature;  $c_4$  is the parameter. (which is 0.037 here

for ordinary concrete), for high-performance concrete (HPC) concrete  $c_4 = 0.017$ .

The compression stress–strain relationship of post-fire concrete can be expressed as

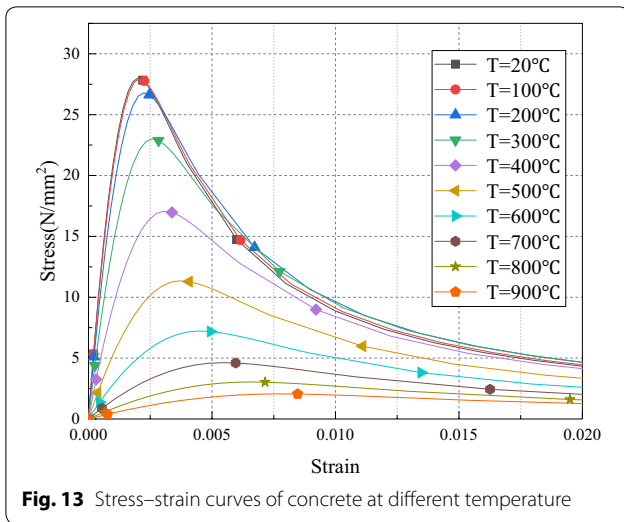


**Fig. 13** Stress–strain curves of concrete at different temperature

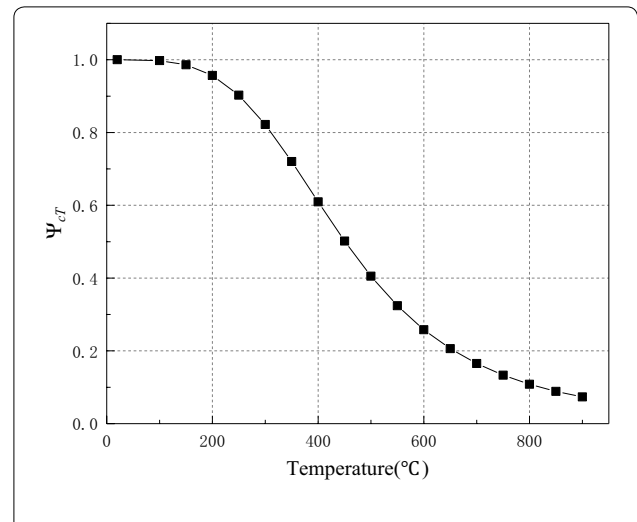


**Fig. 14** Reduction factor of concrete compressive strength

$$y = \begin{cases} \frac{9.1f_{cu}^{-4/9}x-x^2}{1+(9.1f_{cu}^{-4/9}-2)x} & x \leq 1 \\ \frac{x}{2.5 \times 10^{-5}f_{cu}^3(x-1)^2+x} & x > 1 \end{cases}, \quad (8)$$

where  $y = \sigma_c/f_c(T)$ ,  $x = \epsilon_c/\epsilon_0(T)$ ,  $\sigma_c$  is the compressive stress of post-fire concrete, N/mm<sup>2</sup>;  $\epsilon_c$  is the compressive strain of post-fire concrete;  $f_{cu}$  is the cube crushing

$$\frac{E_s(T)}{E_s} = \begin{cases} 1 & T \leq 350^\circ\text{C} \\ 1.0072 - 2.014 \times 10^{-7}T^2 + 5 \times 10^{-5}T & T > 350^\circ\text{C} \end{cases}, \quad (11)$$

strength of concrete at room temperature, N/mm<sup>2</sup>.

The elastic modulus of post-fire concrete  $E_c(T)$  (N/mm<sup>2</sup>) at  $T$  °C is

$$E_c(T) = \frac{E_c}{1 + 2.15 \times 10^{-3}[(T - 20)/800]^{4.33} + 3.7 \times 10^{-2}[(T - 20)/100]^2}, \quad (9)$$

where  $E_c$  is the elastic modulus of concrete at room tem-

### 4.3.2 Constitutive Model of Reinforcement at High Temperature

The built-in bilinear kinematic reinforcement model of Abaqus was used to simulate reinforcement steel, and the elastic modulus  $E_s(T)$  (N/mm<sup>2</sup>) at  $T$  °C proposed by Yu et al. (2005a, b) can be calculated as follows:

where  $E_s$  is the elastic modulus of reinforcement at room temperature, N/mm<sup>2</sup>.

The yield strength reduction factor of reinforcement

$$\Psi_{yT} = \frac{f_y(T)}{f_y} = \begin{cases} 1 & 0^\circ\text{C} < T \leq 200^\circ\text{C} \\ 1.33 - 1.64 \times 10^{-3}T & 200^\circ\text{C} < T \leq 700^\circ\text{C} \end{cases}, \quad (12)$$

perature, N/mm<sup>2</sup>.

The tensile strength of post-fire concrete was calculated by a bilinear model proposed by Hu et al. (2014).

The tensile strength of post-fire concrete  $f_t(T)$  (N/mm<sup>2</sup>) at  $T$  °C is

$\Psi_{yT}$  at  $T$  °C proposed by Miao et al. (2013) is as follows:

where  $f_y(T)$  is the post-fire yield strength of reinforcement, N/mm<sup>2</sup>;  $f_y$  is the yield strength of reinforcement at room temperature, N/mm<sup>2</sup>.

The stress–strain model of reinforcement at high temperature is shown as follows (Fig. 15).

$$\frac{f_t(T)}{f_t} = 0.976 + \left[ 1.56 \times \left(\frac{T}{100}\right) - 4.35 \times \left(\frac{T}{100}\right)^2 + 0.345 \times \left(\frac{T}{100}\right)^3 \right] \times 10^{-2} \quad 20^\circ\text{C} \leq T \leq 800^\circ\text{C}. \quad (10)$$

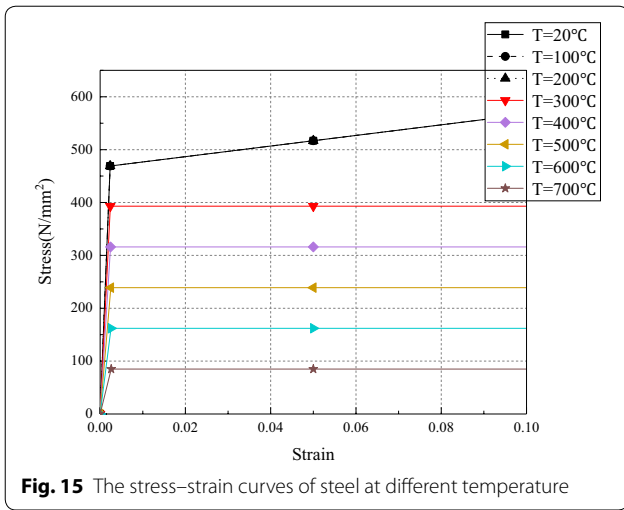


**Fig. 15** The stress–strain curves of steel at different temperature

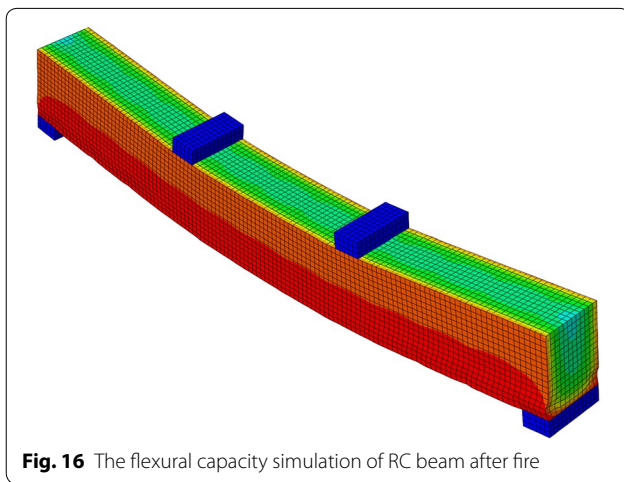


**Fig. 16** The flexural capacity simulation of RC beam after fire

### 4.3.3 Modelling Process

When the beams were simulated using ABAQUS, the constitutive relations of concrete and reinforcement under high temperature (as shown in Figs. 13 and 15) were input into the model. The contact between reinforcement and concrete was simulated through Embedded Region (Fu 2012, Fu et al. 2008). The heat transfer analysis was first performed. Then the result file (.odb) of the heat transfer simulation results was imported into the predefined fields, the loads and analytical steps were followed. The mesh size was 10 mm, in which the concrete was set as C3D8R 8-node linear hexahedron units, while the reinforcement as T3D2 2-node linear 3-dimensional truss units. After submitted the job, the results are provided in Fig. 16. Finally, based on the post-processing function of the software, the post-fire load–deflection curves of the beams were plotted (Fig. 17).

### 4.3.4 FE Model Validation

After RC beams was simulated in ABAQUS, the simulated and tested results of the post-fire flexural capacity of RC beams were compared, the simulated results were basically consistent with the test results.

## 5 Parametric Analysis

The effects of concrete cover thickness ( $c$ ), fire exposure time ( $t$ ), the ratio of longitudinal reinforcement ( $\rho$ ), the fire sides ( $n$ ), and the ratio of shear span to effective depth ( $\lambda$ ) on the post-fire load-bearing ability were investigated using the validated model. Among them, the treatment of the cover thickness is achieved by fine-tuning (increasing 10 mm and decreasing 10 mm) the height of the beam section ( $h$ ) on the basis

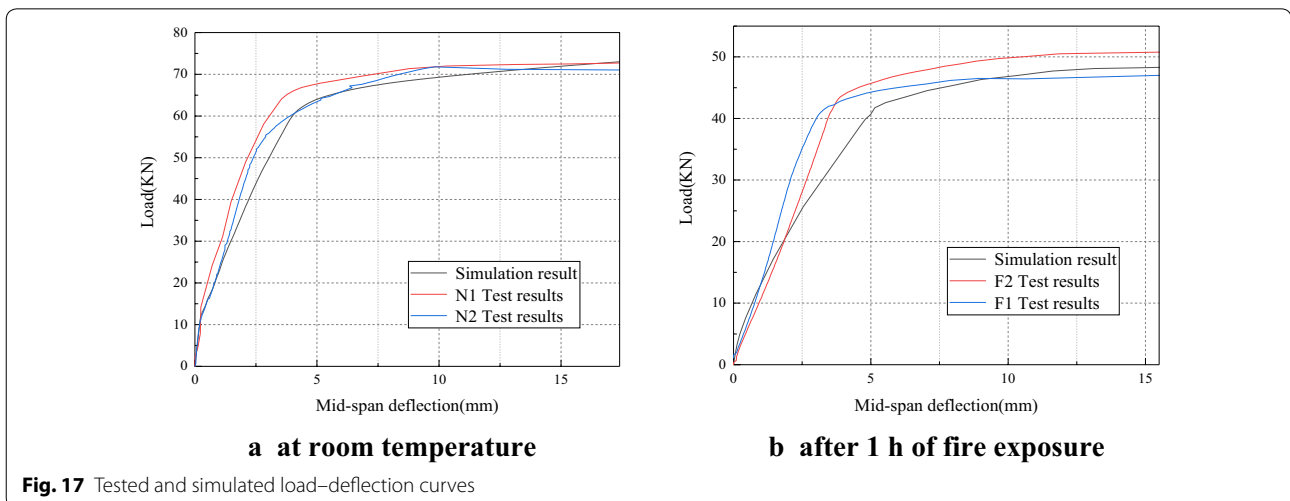
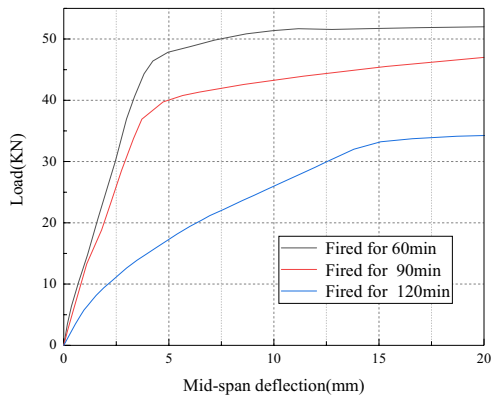
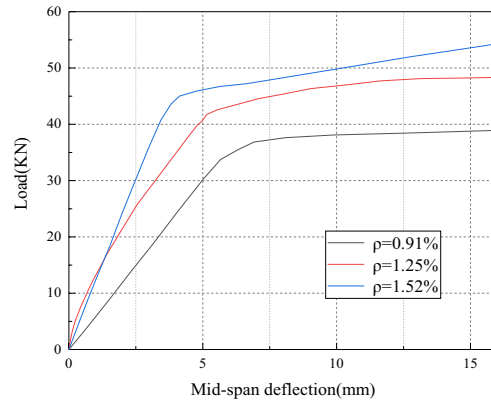


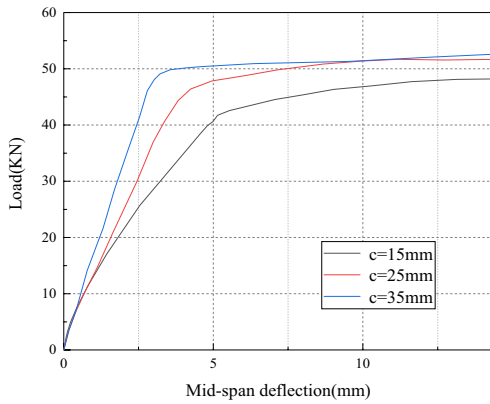
**Fig. 17** Tested and simulated load–deflection curves



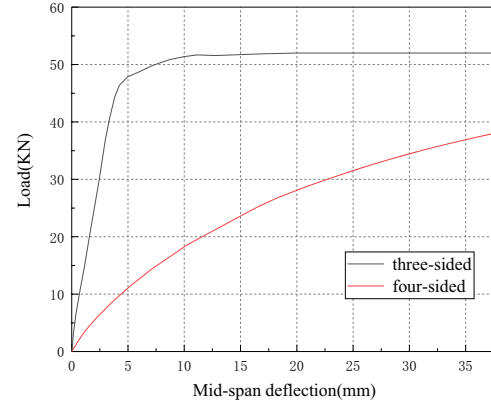
**a load-deflection curves of different fire exposure time**



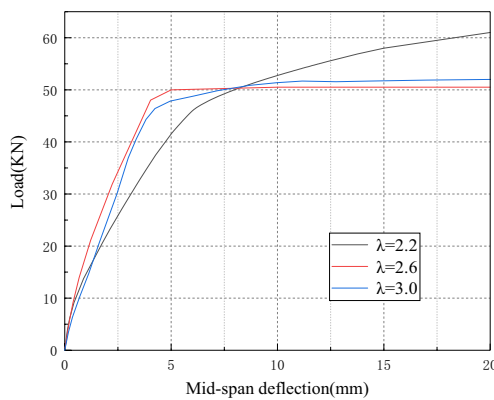
**b load-deflection curves of different reinforcement ratios**



**c load-deflection curves of different cover layer thicknesses**



**d load-deflection curves of different fire sides**



**e load-deflection curves of different ratio of shear span to effective depth**

**Fig. 18** Variation of load–flexural capacity of beams under different parameters

of ensuring that the effective height ( $h_0$ ) of the beam section remains unchanged. Thereby, the finite-element analysis of these factors on the flexural capacity of RC beams can be clarified. The concrete cover thickness was 15, 25 or 35 mm; the fire exposure time was 60, 90 or 120 min; the longitudinal reinforcement ratio was 0.91%, 1.25% or 1.52%, the fire sides was 3 or 4, the ratio of shear span to effective depth was 2.2, 2.6, or 3.0. The analytical results are presented in Fig. 18. To study the effect of the thickness of the concrete cover, the height of the section is adjusted by fine-tuning (increasing and decreasing 10 mm) the cross-sectional dimensions of the beam to ensure that the effective height of the beam section remains unchanged.

Clearly, the flexural capacity of RC beams was significantly weakened after the fire exposure, and the weakening was more obvious with the prolonging of fire exposure time. After the fire exposure, the cover layer thickness directly decided the temperature at the bottom of the tensile reinforcement, and with the larger cover layer thickness, the temperature at the bottom of the steels was lower and the mechanical performance was higher, leading to higher bearing capacity. The ratio of longitudinal reinforcement also affected the bending bearing capacity, and a larger reinforcement ratio led to a higher bearing capacity. Similarly, the difference in fire sides has a great influence on the bearing capacity of the beam. Compared with the three-sided fire beam, the four-sided fire beam will damage the concrete in the compression zone, resulting in a reduction in the bearing capacity. The ratio of shear span to effective depth has little effect on the residual flexural capacity of the beam after fire.

## 6 Calculation Method for Residual Flexural Capacity of the RC Beams

During the fire, the section temperature is unevenly distributed along the section height, so the distribution of concrete compressive strength after fire is not uniform throughout the section. To calculate the residual flexural capacity of the component after fire, the 500 °C isotherm method is adopted in Eurocode (BSI 2004). Han et al. (2007), Xiang et al. (2010) and Yang et al. (2002) used the equivalent section method to determine the ultimate flexural capacity of the beam under fire. This paper propose a new calculation model based on the FEA results and the improved section method to calculate the residual flexural capacity of the post-fire RC beams aiming at refining the flexural capacity calculation with the accurate inclusion of defects of strength reduction of the components caused by fire.

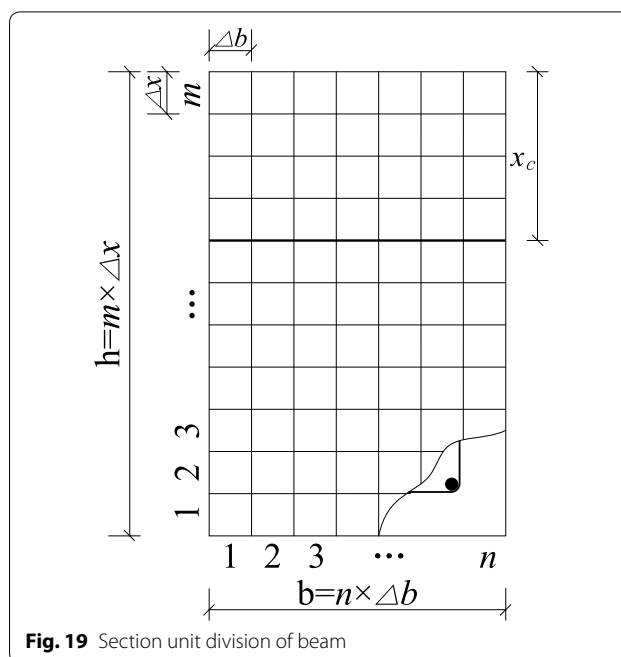


**Fig. 19** Section unit division of beam

### 6.1 Basic Assumptions

Before the calculation, the following basic assumptions are made for the RC beams after fire:

1. The concrete strength of each grid in the compression zone was different, but the strength within each grid was considered as the same;
2. The contribution of concrete in the tension zone to the residual flexural capacity was ignored;
3. There was no relative slip between steel and concrete during the fire;
4. The effect of temperature–stress on the strength of the concrete at high temperature was not considered.

### 6.2 The Limitation of this Method

1. Ignore the effect of fine-tuning the cross-sectional size of the beam on the bending capacity of the beam.
2. It may require longer time period to predict flexural capacity than the existing 500 °C isotherm method from Eurocode.

### 6.3 Calculation Steps

The beam section is meshed. The temperature of each cell can be extracted by the post-processing function of the ABAQUS from thermal analysis model. As shown in Fig. 19, the temperature of concrete after the fire takes the highest temperature  $T_i$  in the  $i$ th cell. The

compressive strength reduction factor of concrete is obtained by substituting  $T_i$  into Eq. 6. The temperature of the steel bar after the fire takes the highest temperature of the cell, where the steel is located. Equation (12) for the yield strength of the steel bar after high temperature is adopted.

According to the strength reduction model of the concrete after high temperature in Fig. 14, the post-fire residual flexural capacity is determined using the improved section method. The height of the compressive zone ( $x_c$ ) of the concrete beam section after the fire can be calculated based on Eq. (13):

$$f_c \sum \Psi_{cTi} \Delta b \Delta x + \Psi'_{yT} f'_y A'_s = \Psi_{yT} f_y A_s, \quad (13)$$

where  $\Psi_{cTi}$  is the compressive strength reduction factor of the  $i$ th cell,  $\Delta b$  is the width of a single cell,  $\Delta x$  is the height of a single cell,  $\Psi'_{yT}$  is the yield strength reduction factor of compressive steel,  $f'_y$  is the yield strength of compressive steel at room temperature, N/mm<sup>2</sup>,  $A'_s$  and

$A_s$  is the area of steel in the compressive and tensile zone, respectively, mm<sup>2</sup>.

The strength reduction factor of concrete in the compressive zone ( $\bar{\Psi}_{cT}$ ) is obtained from Eq. (14):

$$\bar{\Psi}_{cT} = \frac{\sum \Psi_{cTi} \Delta b \Delta x}{bx_c}, \quad (14)$$

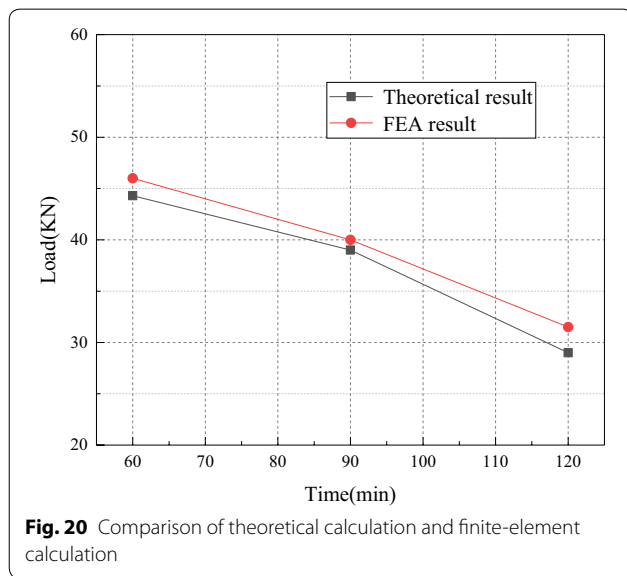
where  $b$  is the width of the beam section,  $x_c$  is the height of the compression zone of the concrete beam section.

After obtaining the height of the compression zone ( $x_c$ ), the residual flexural capacity ( $M_u$ ) of the RC beams after fire can be obtained according to Eq. (15):

$$M_u = \alpha_1 \bar{\Psi}_{cT} f_c b x_c \left( h_0 - \frac{x_c}{2} \right) + \Psi'_{yT} f'_y A'_s (h_0 - a'_s), \quad (15)$$

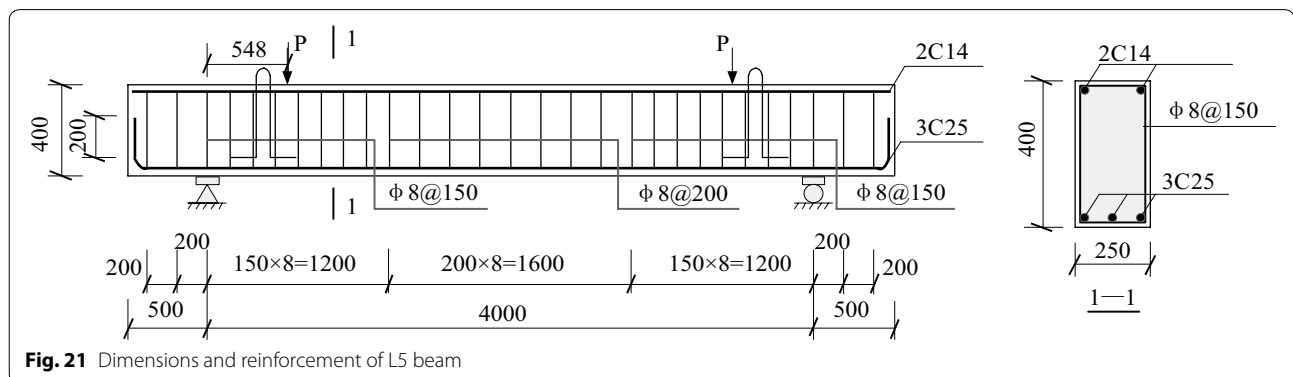
where  $\alpha_1$  is coefficient of equivalent rectangular stress figure in compression zone of concrete, which is 1 here,  $h_0$  is the effective height of the beam section,  $a'_s$  is the distance from the resultant force point of the compressive steel reinforcement to the margins of the compressive section.

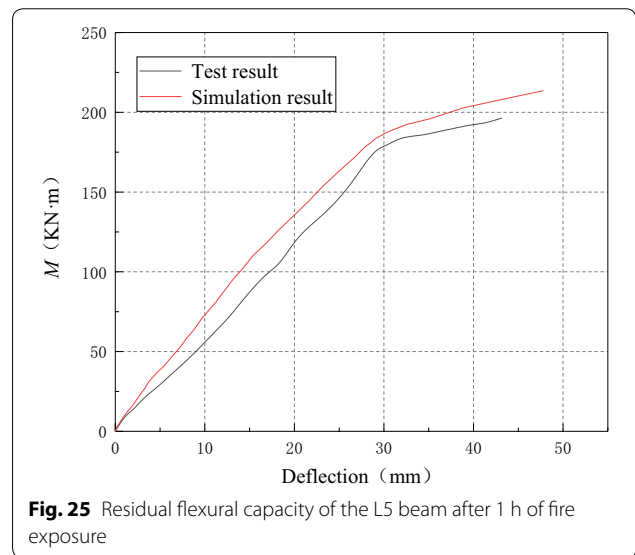
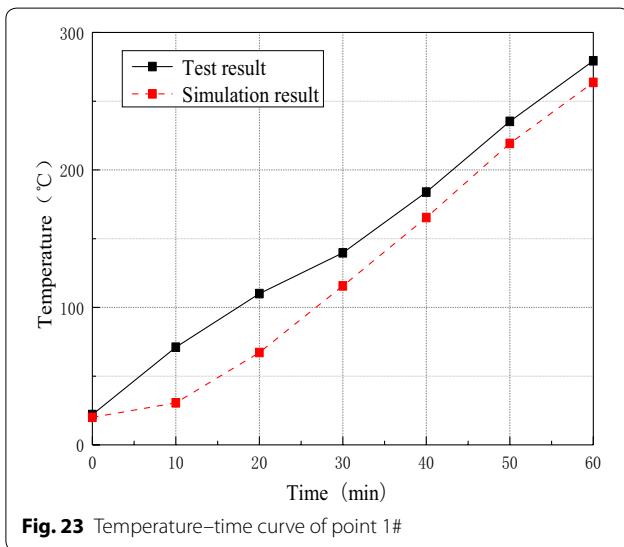
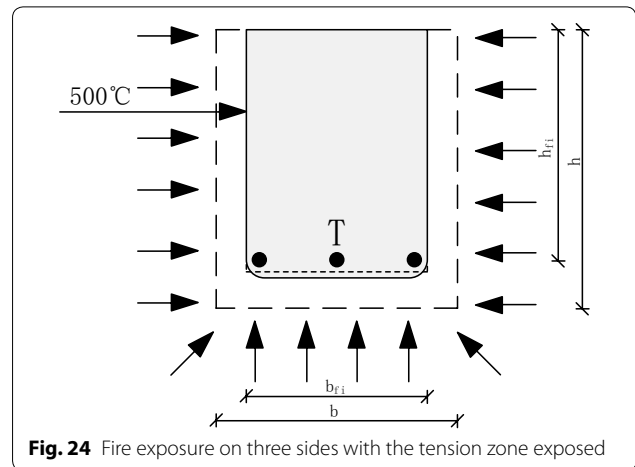
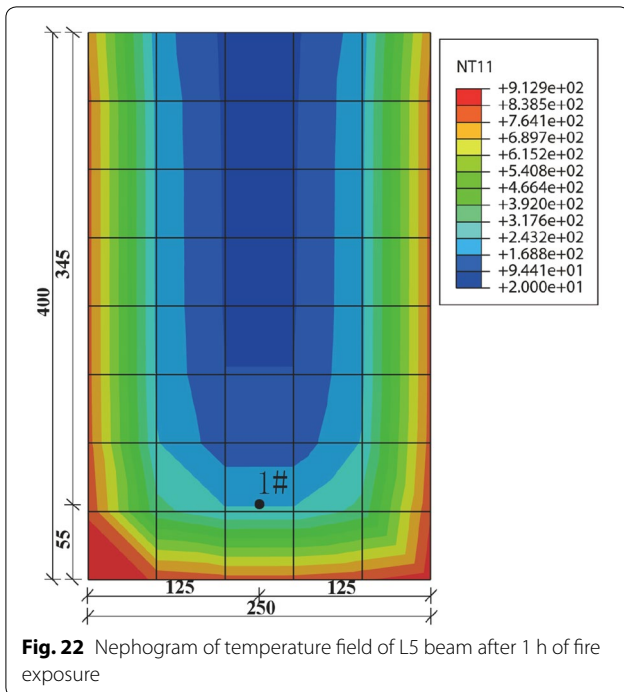
The flexural capacity of the RC beams after 60 min of fire is verified by the above theoretical method, and the flexural capacity after 90 min and 120 min of fire is calculated and compared with the finite-element results. The results are shown in Fig. 20.



#### 6.4 Verification of the Post-fire Flexural Capacity Formula

The test data in Ref. (Xu et al. 2013) of specimen L5 is chosen to validate the correctness and applicability of the theoretical calculation model, and the dimensions and reinforcement of L5 beam is illustrated in Fig. 21. The paper selects temperature measuring point 1# for verification. After the temperature field is simulated using ABAQUS, the nephogram of temperature field is shown in Fig. 22. The comparison between the simulation results and the test results of the Temperature–Time curve of measuring point 1# is shown in Fig. 23.





To more comprehensively compared the accuracy of the improved section method, the 500 °C isotherm method from Eurocode (BSI 2004) is now used to calculate the L5 beam. For a rectangular beam exposed to fire on three-sided, the schematic diagram of effective section of the beam is shown in Fig. 24. In fact, the 500 °C isotherm method is a rough calculation method for the residual flexural capacity of the beam after fire. It is based on the assumption that concrete outside 500 °C no longer provides the bearing capacity of the member, while the

**Table 4** Results of the residual flexural capacity of the L5 beam after 1 h of fire exposure

Method	Result (KN m)	Error (%)
Test	196	–
Simulation	201	2.55
500 °C isotherm	176.77	9.81
Improved section	194.45	0.79

residual concrete maintains its initial values of strength and elastic modulus. On the basic of the above assumptions, after obtaining the 500 °C isotherm, then determine a new width  $b_{fi}$  and a new effective height  $d_{fi}$  of the section by excluding the concrete outside the 500 °C isotherm. The rounded corners of isotherms can be

regarded by approximating the real form of the isotherm to a rectangle or a square. Then determine the reduced strength of the reinforcement according to the temperature of reinforcing bars in the tension and compression zones. Finally, the bending capacity of the beam post-fire can be obtained based on the reduction factor of materials and the formula of bending capacity.

According to the simulation method of the residual flexural capacity of the RC beam after fire in Sect. 4.3, after the simulation of the temperature field of the L5 beam subjected to fire for 60 min, the residual flexural capacity of the L5 beam is now simulated and compared with source test data. The results are shown in Fig. 25. The residual flexural capacity of the L5 beam of the test results of the improved section method results of the simulation results of the 500 °C isotherm method results are summarized in Table 4.

The compressive strength reduction factor and the yield strength reduction factor of the section of beam after fire is determined according to Figs. 14 and 15. The flexural capacity of specimen L5 was calculated with Eqs. (13–15) to be 194.45 kN m, with error 0.79% from that (196 kN m) of specimen L5 in Ref. (Xu et al. 2013) and was calculated with 500 °C isotherm method to be 176.77 kN m with error 9.81%. The flexural capacity of the theoretical calculation model proposed in this paper is well fitted with the Ref. (Xu et al. 2013), which indicates that the method can be applied accurately and effectively to the calculation of the flexural capacity of RC beams after fire.

## 7 Conclusions

The flexural capability of reinforced concrete after fire exposure was simulated on the finite-element analysis software. The proposed theoretical calculation model based on improved section method and EFA was calculated and verified. The following conclusions can be drawn from the above research results.

1. The RC beams can be accurately simulated using the sequential thermo-mechanical coupling model developed in ABAQUS.
2. The fire exposure significantly weakened the flexural capacity and increase the deflection after a longer time of fire exposure.
3. Among the influence factors, the cover thickness, time of fire exposure, the ratio of longitudinal reinforcement, and the ratio of shear span to effective depth all largely affected the flexural capacity of RC beams after fire exposure. The flexural capacity was enhanced with larger cover layer thickness or higher reinforcement ratio but reduced after longer time of fire exposure. The flexural capacity was severely

weakened after four-sided fire. The ratio of shear span to effective depth has little effect on the residual flexural capacity of the beam after fire.

4. The flexural capacity of the post-fire beam obtained by the improved section method was consistent with the results obtained by the FEA software, and it was consistent with the experimental data, and the accuracy was high compared to other methods, which provided reference for the calculation of flexural capacity of RC beams after fire.

### Acknowledgements

This research was financially supported by the Foundation of China Scholarship Council (No. 201805975002), National Natural Science Foundation of China (Grant NO. 51378238), Science and Technological Planning Project of Ministry of Housing and Urban–Rural Development of the People's Republic of China (No. 2017-K9-047). The authors wish to acknowledge the sponsors. However, any opinions, findings, conclusions and recommendations presented in this paper are those of the authors and do not necessarily reflect the views of the sponsors.

### Author's information

BC is a professor affiliated with the University of London and the Jilin Jianzhu University. BL is a master student at the Jilin Jianzhu University. FF is an associate professor at the University of London.

### Authors' contributions

BC and FF designed the research methodology; BL performed the analysis, BL and FF draft the manuscript; BC and FF reviewed the manuscript. All authors read and approved the final manuscript.

### Funding

Founder: Foundation of China Scholarship Council, Award Number No. 201805975002; Founder: National Natural Science Foundation of China, Award Number. 51678274; Founder: Science and Technological Planning Project of Ministry of Housing and Urban–Rural Development of the People's Republic of China, Award Number 2017-K9-047

### Availability of data and materials

The data used to support the findings of this study are available from the authors upon request.

### Competing interests

The authors declare that they have no competing interests.

### Author details

<sup>1</sup> School of Civil Engineering, Jilin Jianzhu University, Changchun 130118, Jilin, China. <sup>2</sup> School of Mathematics, Computer Science and Engineering, City, University of London, London, UK.

Received: 26 December 2019 Accepted: 5 August 2020

Published online: 30 September 2020

### References

- Ban, D. L. (2008). Research on building fire collapse. *Science and Technology Innovation Herald*, 26, 169–170.
- Bratina, S., Planinc, I., Saje, M., & Turk, G. (2003). Non-linear fire-resistance analysis of reinforced concrete beams. *Structural Engineering and mechanics*, 16(6), 695–712.
- BS 5950-8:2003 (Superseded, Withdrawn) Structural use of steelwork in building. Code of practice for fire resistant design
- BSI. (2004). BS EN 1992-1-2: 2004, Eurocode 2—Design of concrete structures—part 1–2: General rules—structural fire design. Structural fire design. London: BSI.



- Chen, Y. H., Chang, Y. F., Yao, G. C., & Sheu, M. S. (2009). Experimental research on post-fire behaviour of reinforced concrete columns. *Fire Safety Journal*, 44(5), 741–748.
- Cheng, S. P. (2007). *Finite element analysis of temperature field and temperature stress of concrete structure*. Doctoral dissertation. Chongqing University.
- Di Capua, D., & Mari, A. R. (2007). Nonlinear analysis of reinforced concrete cross-sections exposed to fire. *Fire Safety Journal*, 42(2), 139–149.
- Eamon, C. D., & Jensen, E. (2013). Reliability analysis of reinforced concrete columns exposed to fire. *Fire Safety Journal*, 62, 221–229.
- El-Hawary, M. M., Ragab, A. M., El-Azim, A. A., & Elibiari, S. (1997). Effect of fire on shear behaviour of RC beams. *Computers & Structures*, 65(2), 281–287.
- Fu, F. (2012). Response of a multi-storey steel composite building with concentric bracing under consecutive column removal scenarios. *Journal of Constructional Steel Research*, 70, 115–126.
- Fu, F. (2016a). 3D finite element analysis of the whole-building behavior of tall building in fire. *Advances in Computational Design*, 1(4), 329–344.
- Fu, F. (2016b). Structural analysis and design to prevent disproportionate collapse, CRC Press ISBN 978-1-4987-8820-5.
- Fu, F. (2018). Design and Analysis of Tall and Complex Structures. Butterworth-Heinemann, ELSEVIER, ISBN 978-0-08-101121-8.
- Fu, F. (2020). Fire induced progressive collapse potential assessment of steel framed buildings using machine learning. *Journal of Constructional Steel Research*, 166, 105918.
- Fu, F., Lam, D., & Ye, J. (2008). Modelling semi-rigid composite joints with precast hollowcore slabs in hogging moment region. *Journal of Constructional Steel Research*, 64(12), 1408–1419.
- Fu, F., Lam, D., & Ye, J. (2010). Moment resistance and rotation capacity of semi-rigid composite connections with precast hollowcore slabs. *Journal of Constructional Steel Research*, 66(3), 452–461.
- Fu, C. G., Liu, W., Kong, W. Y., & Wang, Y. Z. (2015). The temperature field analysis of reinforced concrete beam based on heating and cooling whole curve. *Journal of Shandong Jianzhu University*, 30(4), 307–317.
- Han, Y. L., Wang, Z. Q., Wang, Y. J., & Bai, L. L. (2007). Analysis of bending capability of a reinforced concrete beam supported at both ends in fired field. *Journal of Naval University of Engineering*, 19(1), 76–80.
- Hassan, A., Aldhafairi, F., Abd-EL-Hafez, L. M., & Abouelezz, A. E. Y. (2019). Retrofitting of different types of reinforced concrete beams after exposed to elevated temperature. *Engineering Structures*, 194, 420–430.
- Hu, C. P., Xu, Y. Y., Luo, Y., Zheng, Y. L., & Lin, B. L. (2014). Experimental study on the tensile strength of concrete after high temperature. *Journal of Huaqiao University (Natural Science)*, 35(2), 196–201.
- Hu, Q., Xu, M. X., & Zheng, W. Z. (2006). Estimation method for normal section load-flexural capacity of concrete members subjected to fire. *Journal of Harbin Institute of Technology*, 38(1), 56–58.
- ISO (International Organisation for Standardisation). (1999). ISO 834-1: Fire resistance tests-Elements of building construction. Part 1: general requirements. Geneva: ISO.
- Jiang, F. G., Chen, H., & Bai, L. L. (2008). Analysis and calculation of residual bearing capacity of reinforced concrete beams after fire. *Concrete*, 000(002), 57–59.
- Kodur, V. K. R., & Agrawal, A. (2017). Effect of temperature induced bond degradation on fire response of reinforced concrete beams. *Engineering Structures*, 142, 98–109.
- Liao, J. H., Lu, Z. D., & Su, L. (2013). Experimental and finite element analysis of shear strength of concrete beams subjected to elevated temperature. *Journal of Tongji University (Nature Science)*, 41(6), 806–812.
- Lie, T. T., & Irwin, R. J. (1993). Method to calculate the fire resistance of reinforced concrete columns with rectangular cross section. *ACI Structural Journal*, 90(1), 52–60.
- Lu, Z. D., Zhu, B. L., & Zhou, Y. H. (1993). Experimental study on fire response of simple supported reinforced concrete beams. *China Civil Engineering Journal*, 26(3), 47–54.
- Mathew, G., & Joseph, B. (2018). Flexural behaviour of geopolymer concrete beams exposed to elevated temperatures. *Journal of Building Engineering*, 15, 311–317.
- Miao, J. J., Chen, N., Hou, X. Y., Zhu, Q. Q., & Gong, W. (2013). Experimental research and numerical simulation on fire resistance performance of RC beams with damages caused by service loading. *Journal of Building Structures*, 34(03), 1–11.
- Parthasarathi, N., Saraf, D. S., Prakash, M., & Satyanarayanan, K. S. (2019). Analytical and Experimental study of the reinforced concrete specimen under elevated temperature. *Materials Today: Proceedings*, 14, 195–201.
- Shao, H. Y., Zhu, R. X., & Ren, C. X. (2003). Finite element analysis of temperature field and temperature stress field of structure. *Journal of Ningbo University (Nature Science & Engineering)*, 16(1), 57–60.
- Shi, X. D., & Guo, Z. H. (2000). Investigation on the behavior of reinforced concrete at elevated temperature. *China Civil Engineering Journal*, 33(6), 6–16.
- Sun, J. F., Shi, X. D., & Guo, Z. H. (2002). Experimental study on the mechanical behavior of three-sided heated reinforced concrete beams at high temperature and after cooling. *Building Structure*, 32(1), 34–36.
- Tian, M. G. (2002). *Research and application of damage assessment of reinforced concrete structure after fire*. Doctoral dissertation. Hunan University.
- Wang, Z. Q., & He, J. (2009). *Nonlinear analysis of reinforced concrete structures*. Harbin: Harbin Institute of Technology Press.
- Xiang, K., Wang, G. H., Yu, J. T., Wang, S., & Diao, X. L. (2010). Uniform calculating method of flexural capacity for fire-damaged reinforced concrete bending members. *Fire Science and Technology*, 29(12), 1035–1039.
- Xu, Q., Han, C., Wang, Y. C., Li, X., Chen, L., & Liu, Q. (2015). Experimental and numerical investigations of fire resistance of continuous high strength steel reinforced concrete T-beams. *Fire Safety Journal*, 78, 142–154.
- Xu, Y. Y., Wu, B., Wang, R. H., Jiang, M., & Luo, Y. (2013). Experimental study on residual performance of reinforced concrete beams after fire. *Journal of Building Structures*, 34(8), 20–29.
- Yang, J. P., Shi, X. D., & Guo, Z. H. (2002). Simplified calculation of ultimate load flexural capacity of reinforced concrete beams under high temperature. *Industrial Construction*, 32(3), 26–28.
- Yu, Z. W., Ding, F. X., & Luo, J. P. (2005a). Experimental research on mechanical properties of different type of concrete after high temperature. *Journal of Safety and Environment*, 5(5), 1–6.
- Yu, Z. W., Wang, Z. Q., & Shi, Z. F. (2005b). Experimental research on material properties of new three-grade steel bars after fire. *Journal of Building Structures*, 26(02), 112–116.
- Zeng, Y. F. (2006). *Study on damage assessment and identification of reinforced concrete structure after fire*. Doctoral dissertation. Chongqing University.
- Zhao, M. M. (2014). *Discussion on temperature stress characteristics of concrete*. Doctoral dissertation. Tianjin University.

## Publisher's Note

Springer Nature remains neutral with regard to jurisdictional claims in published maps and institutional affiliations.

Submit your manuscript to a SpringerOpen® journal and benefit from:

- Convenient online submission
- Rigorous peer review
- Open access: articles freely available online
- High visibility within the field
- Retaining the copyright to your article

Submit your next manuscript at ► [springeropen.com](https://www.springeropen.com)